A Dynamic cpSRP43-Albino3 Interaction Mediates Translocase Regulation of Chloroplast Signal Recognition Particle (cpSRP)-targeting Components*[S]

Nathaniel E. Lewis[‡1], **Naomi J. Marty**[‡1], **Karuppanan Muthusamy Kathir**[§], **Dakshinamurthy Rajalingam**[§], **Alicia D. Kight**[‡], **Anna Daily**[§], **Thallapuranam Krishnaswamy Suresh Kumar**[§], **Ralph L. Henry**[‡2], **and Robyn L. Goforth**[‡3]

From the Departments of ‡*Biological Sciences and* §*Chemistry and Biochemistry, University of Arkansas, Fayetteville, Arkansas 72701*

The chloroplast signal recognition particle (cpSRP) and its receptor, chloroplast FtsY (cpFtsY), form an essential complex with the translocase Albino3 (Alb3) during post-translational targeting of light-harvesting chlorophyll-binding proteins (LHCPs). Here, we describe a combination of studies that explore the binding interface and functional role of a previously identified cpSRP43-Alb3 interaction. Using recombinant proteins corresponding to the C terminus of Alb3 (Alb3-Cterm) and various domains of cpSRP43, we identify the ankyrin repeat region of cpSRP43 as the domain primarily responsible for the interaction with Alb3-Cterm. Furthermore, we show Alb3-Cterm dissociates a cpSRP·LHCP targeting complex *in vitro* and stimulates GTP hydrolysis by cpSRP54 and cpFtsY in a strictly cpSRP43-dependent manner. These results support a model in which interactions between the ankyrin region of cpSRP43 and the C terminus of Alb3 promote distinct membrane-localized events, including LHCP release from cpSRP and release of targeting components from Alb3.

Mitochondrial inner membranes and chloroplast thylakoid membranes are densely populated with protein complexes vital to the production of metabolic energy. For both membrane systems, biogenesis requires specialized protein sorting and integration systems, which localize nucleus- and organelle-encoded proteins to the target membrane. Consistent with the prokaryotic origin of mitochondria and chloroplasts, protein insertion into their energy-generating membranes is accomplished via the action of Oxa1p and Albino3 (Alb3), respectively, which belong to a family of protein insertases that includes YidC in bacteria (1–6).

Although YidC/Oxa1p/Alb3 homologues vary dramatically in length (225–795 residues), all share a conserved hydrophobic core of about 200 residues (2) that extends across five transmembrane domains leaving the C terminus exposed to the cytoplasm, matrix, or stroma, respectively. Complementation studies demonstrated that the core regions of both Oxa1p and Alb3 functionally replace the core of YidC to insert membrane proteins via a "YidC only" pathway (7, 8). Similarly, a chimera of YidC fused with the C-terminal ribosome-binding domain of Oxa1p was useful in demonstrating that the core region of YidC can functionally replace the core region of Oxa1p (9). These experimental results show that the core regions of YidC/Oxa1p/Alb3 are at least partially interchangeable and house the capacity for assisting membrane protein transition into adjacent bilayers. They also support the possibility that a conserved function of the YidC/Oxa1p/Alb3 C terminus is to bind soluble targeting machinery. For example, the hydrophilic C-terminal extension of Oxa1p forms an α-helical domain essential for interacting with the ribosome during cotranslational integration (10, 11). Like Oxa1p, Alb3 contains a hydrophilic C-terminal extension that may play a critical role in protein targeting (12, 13). Alb3 works in conjunction with a post-translational chloroplast signal recognition particle (cpSRP)[4] targeting system to integrate a family of nuclearly encoded light-harvesting chlorophyll-binding proteins (LHCPs) into thylakoid membranes where they are assembled with chlorophyll to form light-harvesting complexes (14–17). Antibody binding to the C terminus of Alb3 inhibits LHCP integration and prevents an Alb3-cpSRP interaction (12), suggesting interactions with the C terminus of Alb3 may be required in the cpSRP-dependent targeting reaction.

cpSRP is a heterodimer composed of a highly conserved 54-kDa GTPase (cpSRP54) and a 43-kDa protein (cpSRP43) unique to chloroplasts (18–20). LHCP precursors imported into the chloroplast stroma from the cytosol are N-terminally processed and bound by cpSRP to form a soluble cpSRP·LHCP complex, termed transit complex, which maintains mature-sized LHCP in an integration-competent state (19, 21). Transit complex interacts with a thylakoid membrane-associated SRP receptor GTPase (cpFtsY) prior to interaction with Alb3 (12).

[4] The abbreviations used are: cpSRP, chloroplast signal recognition particle; SRP, signal recognition particle; Alb3-Cterm, 13-kDa fragment corresponding to the C terminus of Albino3; Ank, ankyrin domain; CD, chromodomain; Chl, chlorophyll; cpFtsY, chloroplast FtsY; GMP-PNP, 5′-guanyl-imido-diphosphate trisodium salt; ITC, isothermal titration calorimetry; L18, 18-amino acid peptide corresponding to the cpSRP43-binding site in LHCP; LHCP, light-harvesting chlorophyll-binding protein; SW, salt-washed; IPTG, isopropyl 1-thio-β-D-galactopyranoside; P$_i$, inorganic phosphate.

Although the membrane-localized steps are not well understood, a mechanism must exist for the regulated transfer of LHCP from cpSRP to Alb3 and most likely involves the cpSRP54/cpFtsY GTP hydrolysis cycle. By analogy to cotranslational SRP targeting mechanisms, LHCP release from cpSRP is presumably accompanied by reciprocal GTP hydrolysis by cpSRP54 and cpFtsY to stimulate their release from each other and from Alb3, ensuring their availability for subsequent rounds of targeting.

cpSRP-dependent targeting of LHCPs is novel in that it functions post-translationally, targeting fully synthesized substrates. All other known SRP targeting systems are cotranslational and utilize the translating ribosome as a regulator of substrate binding, GTP hydrolysis, and protein-protein interactions (22, 23). The evolutionary acquisition of cpSRP43 appears critical for post-translational targeting of LHCPs (24). cpSRP43 not only binds targeting substrate (LHCP) but was recently shown to provide both novel and specific chaperone function, capable of independently reversing aggregation of the highly hydrophobic LHCPs (25, 26). Furthermore, cpSRP43 interacts with cpSRP54 and specifically copurifies Alb3 from isolated thylakoid membranes (24, 27–30). More recently, it was found that cpSRP43 binding to Alb3 is mediated by the Alb3 C terminus (13). However, the physiological significance of this low affinity interaction (9.7 μM) remains uncertain.

cpSRP43 is composed of two types of characteristic protein-protein interaction domains: chromodomains (CD) and ankyrin (Ank) repeats (arranged CD1-Ank1-Ank2-Ank3-Ank4-CD2-CD3; Fig. 2) (27, 30). A conserved motif in LHCP, L18, is bound by the Ank repeat region of cpSRP43 (27, 28, 30–32), and cpSRP54 is bound by CD2 (27, 33, 34). As expected, these regions are critical for formation of transit complex (Ank1-CD2), LHCP integration (CD1-CD2), and regulation of GTP hydrolysis (CD1) (27). Although Falk *et al.* (13) suggest that CD2-CD3 are responsible for cpSRP43 binding to the C terminus of Alb3, the physiological contribution of this interaction in the LHCP targeting mechanism is not known, and CD3 can be removed from cpSRP43 without consequence to the efficiency of transit complex formation or LHCP integration into isolated thylakoids (27).

Although key LHCP targeting/insertion components and transit of LHCP through the stroma to the thylakoids have been examined in detail, many questions remain concerning the orchestration and timing of membrane-associated cpSRP-dependent targeting events. Results described in this study indicate that the Ank repeat domain of cpSRP43 is responsible for high affinity binding to Alb3-Cterm (97 nM) with CD2 contributing slightly to the binding interface. We show that this interaction is functionally critical for efficient assembly of a cpSRP·cpFtsY·Alb3 membrane complex and is used in LHCP targeting to regulate the timing of GTP hydrolysis by cpSRP54/cpFtsY. Our data also indicate that cpSRP43 binding to Alb3-Cterm affects the stability of transit complex, which supports a role of this interaction in promoting release of LHCP from cpSRP at the thylakoid membrane. Collectively, our results support a model whereby cpSRP43 targets available Alb3 via its C terminus and communicates this interaction to cpSRP/cpFtsY thereby triggering downstream events (*e.g.* GTP hydrolysis and

substrate release) required to promote LHCP integration into the thylakoid membrane.

EXPERIMENTAL PROCEDURES

All reagents, enzymes, and primers used were purchased commercially. Plasmids described previously were used for *in vitro* transcription and translation of pLHCP (35), cpSRP43 (36), and cpFtsY (36). Recombinant purified cpSRP43, GST-cpSRP43, GST, GST-Ank1-CD2, GST-CD1, GST-CD2, CD2, ΔCD1, ΔCD2, and ΔCD3 were prepared as described previously (27). His-cpSRP43 (24), Trx-His-S_{tag}-cpFtsY (12, 37), and cpSRP54-His (12) were prepared as described with the exception of a new restriction site (XhoI) for cpFtsY. A peptide corresponding to the cpSRP43-binding site in LHCP, L18 (VDPLYPGGSFDPLGLASS), has been previously described (32). Antibodies to the following proteins have also been described as follows: Alb3-Cterm (38), Alb3–50 amino acids (17), cpSRP43 (12), cpFtsY (12), and cpSRP54 (12). All cloned sequences were verified by sequencing.

Construction of Alb3-Cterm Clones—A cDNA clone for PPF1 (defined as Alb3 in *Pisum sativum*) was obtained by RT-PCR using total RNA from *P. sativum*. Forward and reverse primers matching the sequence for PPF1 (accession number Y12618) were designed to include EcoRI and XbaI sites, respectively, for ligation into pGEM-4Z (Promega). The coding sequence for PPF1-Cterm, a 124-amino acid segment of PPF1 beginning at NNVLSTA and ending at SKRKPVA, was amplified by PCR from PPF1-pGEM-4Z. The resulting PCR fragment was restricted with BamHI and XbaI and then ligated into similarly restricted pGEM-4Z to produce the plasmid Alb3-Cterm-pGEM-4Z. Forward and reverse primers were designed to match the beginning and ending of the Alb3-Cterm and to include SphI and HindIII sites, respectively, for ligation into pQE-80L (Qiagen). The forward primer also included a two amino acid linker (SA), a FLAG™ tag, and a Thrombin cleavage site. The resulting PCR fragment was restricted with SphI and HindIII and then ligated into similarly restricted pQE-80L to create the plasmid His-FLAG-Alb3-Cterm-pQE-80L. This plasmid was transformed into BL21 Star (Invitrogen) and used for IPTG-induced expression of His-FLAG-Alb3-Cterm. All Alb3 constructs are from *P. sativum*.

To produce His-S_{tag}-Alb3-Cterm, His-FLAG-Alb3-Cterm-pQE-80L was amplified by PCR with a reverse primer designed to match the ending of the Alb3-Cterm sequence and a forward primer designed to replace the FLAG tag (DYKDDDDK) with an S tag (KETAAAKFERQHMDS) resulting in a construct with a His$_6$ tag, SA linker, S_{tag}, thrombin cleavage site, and the 124-amino acid segment of PPF1 beginning at NNVLSTA and ending at SKRKPVA. This plasmid, referred to as His-S_{tag}-Alb3-Cterm-pQE-80L, was transformed into BL21 Star and used for IPTG-induced expression of His-S_{tag}-Alb3-Cterm.

Briefly, expressed Alb3-Cterm peptides were affinity-purified over Talon® Superflow metal affinity chromatography and either followed directly by desalting into HKMK (10 mM Hepes-KOH, pH 8.0, 10 mM MgCl$_2$, 100 mM KCl) buffer or followed by a cation exchange step over Resource S (binding: 20 mM Hepes, pH 8, 10 mM KCl, and elution: 20 mM Hepes, pH 8, 1 M KCl) and then desalting into HKMK buffer.

Construction of cpSRP43 Clones—Coding sequences for CD1 and CD2 were amplified by PCR from GST-CD1-pGEX-4T-2 and GST-CD2-pGEX-4T-2 (27) using forward primers designed to incorporate a BamHI restriction site and His$_6$ tag and match the beginning of the CD1 (GEVNKII) or CD2 (QVFEYAE) coding sequences and reverse primers designed to match a pGEX plasmid. Coding sequences for Ank1-CD2 were amplified by PCR from GST-ΔCD3 (27) using forward primers designed to incorporate a BamHI restriction site and a His$_6$ tag and match the beginning of Ank1 (SEYETP) and reverse primers designed to match a pGEX plasmid. PCR products were restricted with BamHI and EcoRI (His-CD1 and His-Ank1-CD2) or XhoI (His-CD2) and ligated into similarly restricted pGEX-6P-2, producing GST-His-CD1-pGEX-6P-2, GST-His-CD2-pGEX-6P-2, and GST-His-Ank1-CD2-pGEX-6P-2. His-CD1, His-CD2, and His-Ank1-CD2 plasmids were transformed into BL21 Star and used for IPTG-induced expression of these constructs as described previously (27). The ΔCD2/CD3 cpSRP43 construct for expression in *Escherichia coli* was produced by PCR amplification of the entire mature cpSRP43-pGEX-6P-2 plasmid (37) minus the codons for amino acids to be deleted (Δ273–377; missing residues AEVDEI…QQPMNE). The use of phosphorylated primers corresponding to the flanking regions of the sequence to be deleted allowed for efficient ligation of the PCR products to re-circularize the plasmid and form the desired coding sequence for GST-ΔCD2/CD3-pGEX-6P-2. This plasmid was transformed into BL21 Star for IPTG-induced expression.

Briefly, expressed GST constructs were affinity-purified by using glutathione-Sepharose™ 4 Fast Flow resin (GE Healthcare) followed by a desalting step into HKM (10 mM Hepes-KOH, pH 8.0, 10 mM MgCl$_2$) buffer as described. Following the glutathione-Sepharose purification, cleaved constructs were brought to 50 mM Tris-HCl, 150 mM NaCl, 1 mM EDTA, 1 mM DTT, pH 7.0, and incubated with PreScission™ protease (GE Healthcare) overnight at 4 °C. Cleaved constructs were desalted into phosphate-buffered saline and passed over glutathione-Sepharose 4 Fast Flow resin for removal of cleaved GST and PreScission™ protease followed by desalting into HKM buffer.

Ank1–4 was amplified from mature cpSRP43 in pGEM-4Z (37) using forward and reverse primers designed to match the beginning (EYETPWW) and ending (RRIGLEKVINV) of Ank1–4 and incorporate BamHI and SalI sites. PCR products were restricted with BamHI and SalI and ligated into similarly restricted pQE-80L, producing His-Ank1–4-pQE-80L. This plasmid was transformed into BL21 Star and used for IPTG-induced expression of His-Ank1–4. His-Ank1–4 was produced as inclusion bodies, solubilized in 8 M urea, and purified as a soluble protein with Talon® Superflow metal affinity resin. His-Ank-1–4 containing 8 M urea was dialyzed against Tris-HCl, pH 7.5, and subsequently buffer exchanged into HKM.

Preparation of Chloroplasts and Radiolabeled Precursors—Intact chloroplasts were isolated from 10- to 12-day-old pea seedlings (*P. sativum* cv. Laxton's Progress) and used to prepare thylakoids and stroma as described previously (39). Chlorophyll (Chl) content was determined as described previously (40). Thylakoids were isolated from lysed chloroplasts by centrifuga-

tion and salt-washed (SW) two times with 1 M potassium acetate in import buffer (IB: 50 mM Hepes-KOH, pH 8.0, 0.33 M sorbitol) and two times with IB with 10 mM MgCl$_2$ (IBM) prior to use. For protease treatment, SW thylakoids were diluted to 0.5 mg/ml Chl in IB with 0.2 mg/ml thermolysin and 1 mM CaCl$_2$ and incubated for 40–60 min (*P. sativum*). Subsequently, samples were combined with EDTA in IB to 20 mM EDTA, and either washed or applied to a 7.5% Percoll™ (GE Healthcare) gradient in IB containing 10 mM EDTA. Pellets from the Percoll gradient were washed once with IB containing 10 mM EDTA and twice with IBM. Protease-treated thylakoids were resuspended at 1 mg/ml Chl in IBM.

In vitro transcribed capped RNA was translated in the presence of [^{35}S]methionine (41) using a wheat germ system to produce radiolabeled proteins (39). Precursor LHCP translation products were diluted 2-fold with 30 mM unlabeled Met in IB. cpSRP43, cpSRP54, and cpFtsY constructs were labeled with ratios of labeled and unlabeled Met such that an equal ^{35}S signal represented equimolar protein as described previously (36). Constructs were quantified by comparing the ^{35}S signal from a given protein band as analyzed by SDS-PAGE and phosphorimaging. Equimolar amounts of proteins were added to each experiment.

Thylakoid Binding Assay—*P. sativum* thylakoid binding assays included SW or protease-treated thylakoids (equal to 75 µg of Chl) in IBM and radiolabeled cpSRP43 or cpFtsY. Reactions were incubated for 30 min in light at 25 °C. Thylakoids were centrifuged at 3200 × g for 6 min, washed in 1 ml of IBM, and transferred to clean tubes. Thylakoids were then pelleted, solubilized in SDS buffer, and heated. Amounts equivalent to 7.5 µg of Chl per sample were analyzed by SDS-PAGE and phosphorimaging.

Protein Binding Assays—Alb3 coprecipitation by cpSRP components was examined by incubating SW thylakoids (equal to 75 µg of Chl) with 10 µg of His-tagged protein and in the presence or absence of 0.5 µM GMP-PNP at 25 °C for 30 min in light. Thylakoids were washed with 600 µl of IBM and solubilized with 2% *n*-dodecyl-β-D-maltoside (maltoside) in IB for 10 min. Samples were centrifuged at 70,000 × g for 12 min, and soluble material was incubated with 50 µl of a 50% Talon Superflow metal affinity resin slurry in IB for 30 min while shaking. Resin was washed three times with 0.1% maltoside in IB and once with IB before elution in 50 µl of SDS sample buffer. Eluted proteins were separated by 12.5% SDS-PAGE and Western blotted for cpSRP43, cpSRP54, cpFtsY, and Alb3. The protein loading control lane is equivalent to 1/100th of the available Alb3 as based on the total amount of thylakoids used.

GST-cpSRP43 constructs/Alb3-Cterm binding assays were performed by incubating 350 pmol (4.7 µM final concentration) of GST-fused cpSRP43 or construct with 1500 pmol (20 µM final concentration) of His-S$_{tag}$-Alb3-Cterm for 15 min at 25 °C and adding 30 µl of a 50% glutathione-Sepharose 4 Fast Flow slurry in 10 mM Hepes-KOH, pH 8.0, 10 mM MgCl$_2$ (HKM), in a final volume of 75 µl. Samples were allowed to mix for 30 min at 4 °C and then transferred to a 0.8-ml centrifuge column (Pierce) and washed three times with 0.75 ml of 20 mM HK, 300 mM KCl, 10 mM MgCl$_2$, 2% Tween 20, three times with 0.75 ml of 0.1% maltoside in IB, and three times with 0.75 ml of HKM.

Coprecipitating proteins were eluted in 75 μl of SDS-PAGE solubilization buffer. Eluted proteins were separated by 12.5% SDS-PAGE and visualized by staining with Coomassie Blue.

Coprecipitation of cpSRP43 and constructs by His-S$_{tag}$-Alb3-Cterm was accomplished by incubating 800 pmol (8 μM final concentration) of Alb3-Cterm with 30 μl of 50% S-protein/agarose slurry (Novagen) in IB and shaking gently for 15 min at 25 °C. After addition of 1500 pmol (15 μM final concentration) of cpSRP43 or construct, in a final volume of 100 μl, samples were allowed to mix for 30 min at 4 °C and then transferred to a 0.8-ml centrifuge column and washed three times with 0.1% maltoside in IB. Coprecipitating proteins were eluted in 75 μl of SDS-PAGE solubilization buffer. Eluted proteins were separated by 12.5% SDS-PAGE and visualized by staining with Coomassie Blue.

Isothermal Titration Calorimetry (ITC)—ITC experiments were performed using a VP-ITC titration microcalorimeter (MicroCal Inc.). All solutions were degassed under vacuum and equilibrated at 25 °C prior to titration. Protein or peptide (50–200 μM) was loaded into the sample cell (1.4 ml), and the titration syringe was loaded with another protein or peptide at 10–30-fold higher concentration. Titrations were routinely carried out using 40–50 injections of 6-μl aliquots using the injection rate of 5–7-min intervals with a stirring rate of 340 rpm. Solutions were prepared either in a buffer containing 10 mM Tris, 100 mM NaCl, pH 7.5, or in HKM. Titration curves were corrected for protein-free buffer and analyzed using Origin ITC software (MicroCal Inc.) (42).

Transit Complex Formation Assays—Transit complex was formed in 60-μl assays by mixing 25 pmol (0.4 μM final concentration) each cpSRP43 and cpSRP54 with 10 μl of diluted translation product similar to assays described previously (32, 43). Assays were incubated for 20 min at 25 °C, and then 0–2000 pmol (0–33.3 μM) of either His-S$_{tag}$-Alb3-Cterm peptide in 20 μl of HKMK, CD3 in HKM, or GST in HKM was added as indicated. Assays were incubated for 20 min at 25 °C and then centrifuged at 70,000 × g for 1 h. The top 30-μl supernatant was removed, cooled on ice, and prepared for native PAGE by the addition of 5 μl of 50% glycerol.

In moving radiolabel assays, transit complex components (cpSRP43, cpSRP54, and LHCP) were all produced by *in vitro* transcription/translation via a wheat germ system. Indicated protein component was translated in the presence of [^{35}S]methionine to produce the radiolabeled protein. The other two components were translated in the presence of nonradioactive Met. Proteins (10 μl of each TP) were then treated as above to form transit complex prior to the addition of 0–5000 pmol (0–83.3 μM) of His-S$_{tag}$-Alb3-Cterm and analysis by native PAGE.

Analysis of Samples—A portion of each sample from each assay was analyzed by SDS-PAGE (or native PAGE as indicated) followed by Western blotting or phosphorimaging. GE Healthcare image analysis software (ImageQuant) was used for quantification of radiolabeled protein from phosphorimages obtained using a Typhoon 8600. Horseradish peroxidase-labeled mouse IgG (Southern Biotech) was used as secondary antibody, and blots were developed with SuperSignal® West Pico chemiluminescent substrate (Pierce). Western blots were imaged using an Alpha Innotech FluorChem IS-8900 using chemiluminescent detection. AlphaEase FC Stand Alone software (Alpha Innotech) was used for quantification. SDS-PAGE standards (Invitrogen) were used to calculate molecular weights (MagicMark^{TM} XP Western Standard for Western blots; Benchmark^{TM} Protein Ladder for Coomassie-stained gels). Protein concentrations were estimated by Coomassie Blue staining.

GTPase Assays—Recombinant cpSRP54 and cpFtsY were assayed for GTPase activity alone or in the presence of recombinant cpSRP43, recombinant cpSRP43 deletion constructs, and/or His-S$_{tag}$-Alb3-Cterm as described previously (27, 44). GTPase activity was measured in solution by determining the amount of inorganic phosphate released by GTP hydrolysis. Assays containing 150 pmol (1 μM final concentration) of cpSRP43 (or indicated construct), cpSRP54, cpFtsY, the indicated amount of His-S$_{tag}$-Alb3-Cterm (0–40 μM, 0–6000 pmol), and 2 mM GTP were brought to a final volume of 150 μl in HKM and incubated at 30 °C for 1 h. After incubation, SDS was added to a final concentration of 6% to denature protein components and prevent subsequent GTPase activity. The addition of ascorbic acid and ammonium molybdate (to 6 and 1%, respectively) was followed by a 5-min incubation, and subsequently each assay was brought to 1% sodium citrate, sodium (meta)arsenite, and acetic acid for a final volume of 1.05 ml. The absorbance of each sample was then measured at 850 nm. Throughout the duration of the experiment, the amount of GTP hydrolyzed increased linearly. Furthermore, a standard curve of inorganic phosphate (P$_i$) was linear from 2 to 75 nmol of P$_i$ and was used to determine the amount of P$_i$ released in each assay. A substrate control that lacked protein components and a zero time control with the protein denatured by the addition of 6% SDS prior to the addition of GTP varied from 0.0 to 2.3 nmol of P$_i$ between experiments and were used to correct for nonspecific hydrolysis and background hydrolysis for each assay.

RESULTS

cpSRP43 Interacts with the Thylakoid Membrane Protein Alb3—We previously demonstrated that His-tagged cpSRP43 binds SW *P. sativum* thylakoid membranes and copurifies Alb3 (24). More recently, it was published that cpSRP43 alone or as a heterodimer with cpSRP54 binds Alb3 through interactions between chromodomains (CDs) at the C terminus of cpSRP43 (CD2 and CD3) and the stroma-exposed C terminus of Alb3 (13). However, the physiological role of cpSRP43 binding to Alb3 is not known. In this context, we asked whether cpSRP43 plays a role in promoting Alb3 association with a cpSRP·cpFtsY complex, which forms at the thylakoid membrane (12). His-tagged cpSRP43, cpSRP54, and cpFtsY constructs shown to be active in reconstituting LHCP integration into isolated thylakoids and able to form a stable complex with Alb3 (12) were incubated with SW thylakoids in the presence or absence of GMP-PNP. Membranes were solubilized with maltoside and then mixed with Talon® Superflow metal affinity resin to repurify His-tagged constructs and associated proteins (Fig. 1*A*). Samples were probed for His-tagged constructs and coprecipitating Alb3 (*P. sativum* PPF1). Assays containing cpSRP54,

A Talon Precipitation

B Alb3 Coprecipitated with His-Constructs
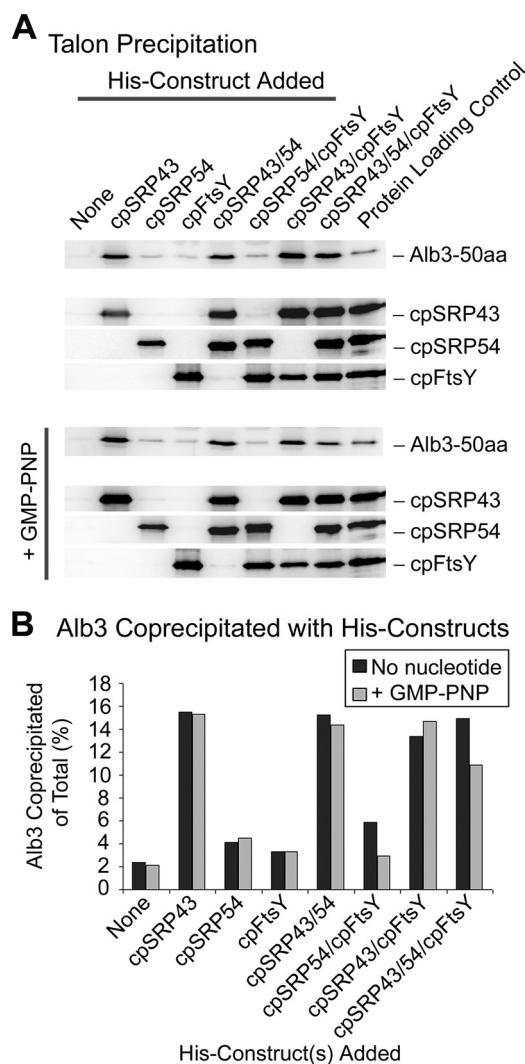
FIGURE 1. **cpSRP43 is the predominant interacting partner with the translocase Alb3 in thylakoids.** *A,* SW thylakoids (75 μg of Chl) were incubated with 10 μg of His-tagged constructs as indicated. Membranes were solubilized and used for purification with Talon Superflow metal affinity resin. Western blots of copurified proteins are shown probed for proteins indicated to the *right. Protein Loading Control* lanes contain thylakoid membranes or 50 ng of His-tagged construct for comparing relative amounts precipitated. *aa,* amino acids. *B, graph* depicts the amount of Alb3 copurified with His-tagged constructs. Total precipitated Alb3 was calculated from the relative signal of total thylakoid lane and eluate lanes in *A.*

cpFtsY, or both copurify ~6% or less of the available Alb3, which is slightly above background binding (~2%) to the resin (Fig. 1, *A* and *B*). In contrast, assays containing cpSRP43 copurify ~15% of the available Alb3 (Fig. 1, *A* and *B*). Similar amounts of each added His-tagged construct were repurified indicating that changes in the amount of copurified Alb3 are not due to inaccessible His tags. The requirement for cpSRP43 to copurify Alb3 suggests that cpSRP43 functions as the bridge that connects cpSRP and cpFtsY to Alb3.

Copurification of Alb3 could stem from interaction of cpSRP43 with an unknown Alb3-associated thylakoid protein or could stem from binding of cpSRP43 to the Alb3 C terminus, an interaction reported recently using recombinant cpSRP43 and protein corresponding to the C terminus of Alb3 (Alb3-Cterm) (13). However, the reported affinity between cpSRP43

and Alb3-Cterm (K_d ~10 μM) seems insufficient to support specific molecular interactions expected for efficient protein targeting and approaches affinity values observed for nonspecific protein interactions (45). To investigate these possibilities further, we tested the ability of cpSRP43 to bind thylakoids lacking the C terminus of Alb3. Alb3 contains five transmembrane domains with its N terminus facing the thylakoid lumen (6). Thermolysin treatment of thylakoid membranes removes the C terminus of Alb3, but otherwise it has no effect on Alb3 integrity as judged by the size of the protease-resistant fragment (~30 kDa), which is detectable with antisera to a protease-resistant, stroma-exposed loop (anti-50 amino acids) and undetectable using antibody against the Alb3 C terminus (supplemental Fig. S1*B*). Although binding of cpFtsY to protease-treated thylakoids is unaffected because of its affinity for thylakoid lipids (36), the ability of cpSRP43 to bind protease-treated thylakoids is diminished by ~80% (supplemental Fig. S1*A*), further supporting a role of the Alb3 C terminus in cpSRP43 binding to thylakoids. Taken together with the results of Fig. 1, these data suggest that one role of cpSRP43 binding to the Alb3 C terminus is to promote efficient formation of a cpSRP·cpFtsY·Alb3 complex.

Ankyrin Region of cpSRP43 Provides the Primary Interface for Binding Alb3-Cterm—To better understand how a low affinity interaction is used to support cpSRP43-Alb3 association, we used ITC to reexamine the binding of cpSRP43 to recombinant Alb3-Cterm expressed and purified from *E. coli.* Surprisingly, ITC demonstrated that the affinity of cpSRP43 for His-FLAG-Alb3-Cterm was in the nanomolar range (94 nM; Fig. 2*A*) as opposed to the micromolar (~10 μM) affinity reported earlier (13). Although the reason(s) for the observed discrepancy in the binding affinity is not clear, systematic examination of the buffer components used by Falk *et al.* (13) to observe micromolar affinity revealed that glycerol (at 5% v/v concentration) contributes significantly to the heat of the reaction and consequently influences the ability to accurately measure the K_d values using binding isothermogram (supplemental Fig. S2). Because ITC conducted in the presence of glycerol had also been used to demonstrate that CD2 and CD3 of cpSRP43 provide the binding interface for Alb3-Cterm, the role of cpSRP43 domains in binding Alb3-Cterm was examined using both ITC in the absence of glycerol and copurification assays.

cpSRP43 domain deletions (Fig. 2*B*) were examined by ITC for their ability to interact with His-FLAG-Alb3-Cterm. Similar to cpSRP43 ($K_{d(\mathrm{app})}$ ~94 nM), His-Ank1-CD2 interacts with a near 1:1 stoichiometry and exhibits a high binding affinity for Alb3-Cterm ($K_{d(\mathrm{app})}$ ~64 nM; Fig. 2*C*). The binding affinity of Alb3-Cterm for His-Ank1–4 (Fig. 2*D*) is marginally lower ($K_{d(\mathrm{app})}$ ~205 nM) than that observed for cpSRP43 or His-Ank1-CD2, but remains in the nanomolar range. In contrast, Alb3-Cterm interaction with CD2 exhibits negligible binding affinity ($K_{d(\mathrm{app})}$ ~350 μM; Fig. 2*E*) as compared with that observed for Alb3-Cterm binding to cpSRP43, His-Ank1-CD2, or His-Ank1–4. In contrast to Falk *et al.* (13), these observations indicate that the binding site for Alb3-Cterm lies in the ankyrin repeat region of cpSRP43 with the second chromodomain possibly adding to the interaction face based on compar-
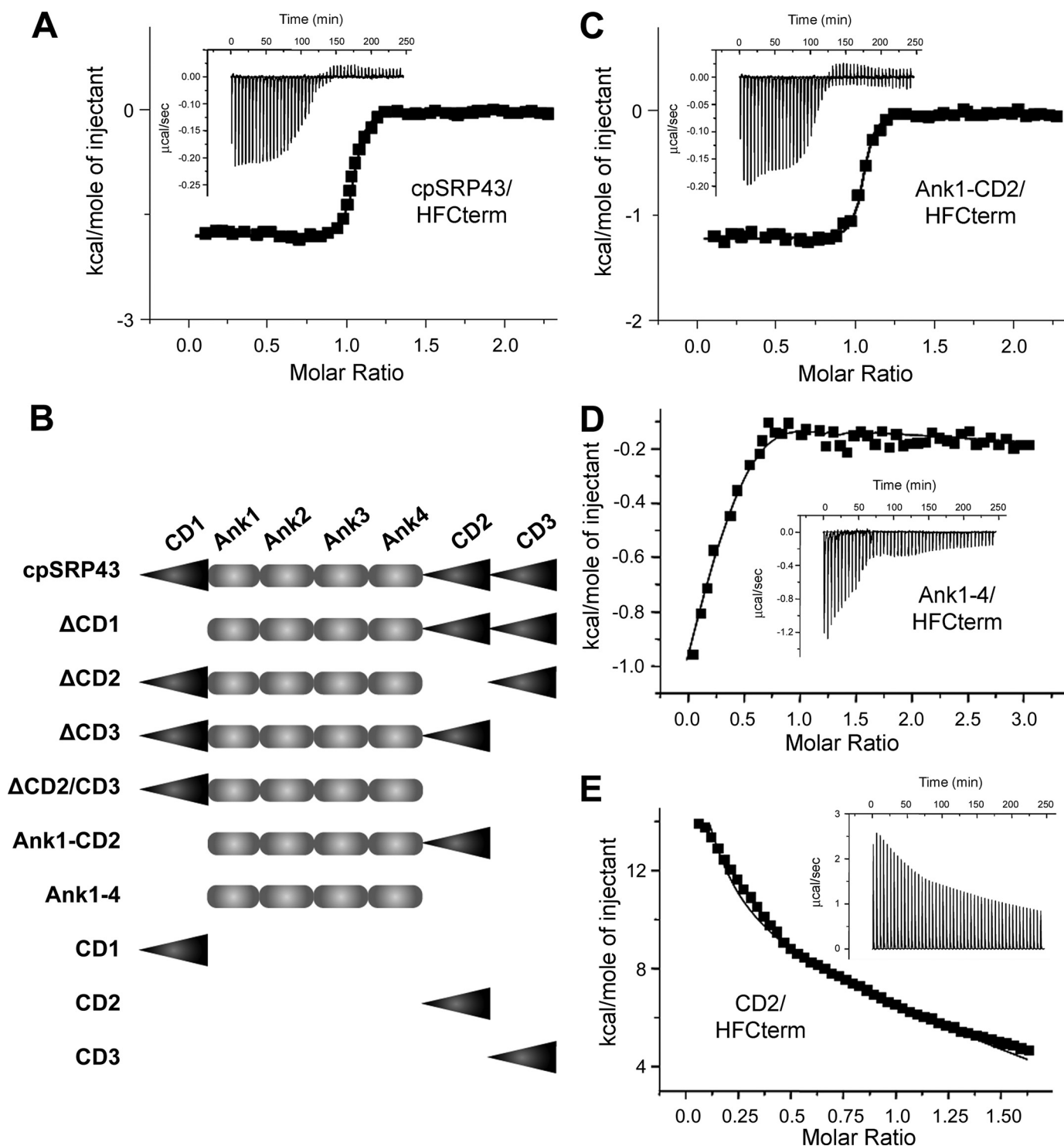
FIGURE 2. **Ankyrin region of cpSRP43 is the interacting domain with the C terminus of Alb3.** *A, C, D,* and *E,* ITC curves showing data characterizing interactions between His-FLAG-Alb3-Cterm with cpSRP43 constructs as indicated. All experiments were done at 25 °C. The *insets* and *larger panels* show the raw and integrated data, respectively, of the titration of cpSRP43 construct with Alb3-Cterm as indicated. The *solid line* in the *larger panels* represents the best fit curve of the data (Microcal Origin). *B,* depiction of the domain organization of cpSRP43, with *triangles* representing chromodomains and *rounded rectangles* representing ankyrins. Domains are listed in the N to C termini order across the *top*. Protein constructs described in this study are shown as listed on the *left*.

ison of the affinity of Alb3-Cterm for His-Ank1–4 and His-Ank1-CD2.

Copurification assays were conducted to confirm and extend the results obtained using ITC. Equimolar concentrations of GST, GST-cpSRP43, GST-Ank1-CD2, GST-CD2, GST-ΔCD2/ CD3, or GST-CD1 (refer to Fig. 2*B*) were incubated with His-

S_{tag}-Alb3-Cterm and recovered using glutathione-Sepharose. Bound proteins were eluted, separated by SDS-PAGE, and visualized directly by staining with Coomassie Blue. GST-cpSRP43 specifically coprecipitates Alb3-Cterm (apparent molecular mass ~20 kDa) at a ratio of ~0.85 pmol of Alb3-Cterm copurified per pmol of cpSRP43 (Fig. 3*A*). GST-tagged constructs
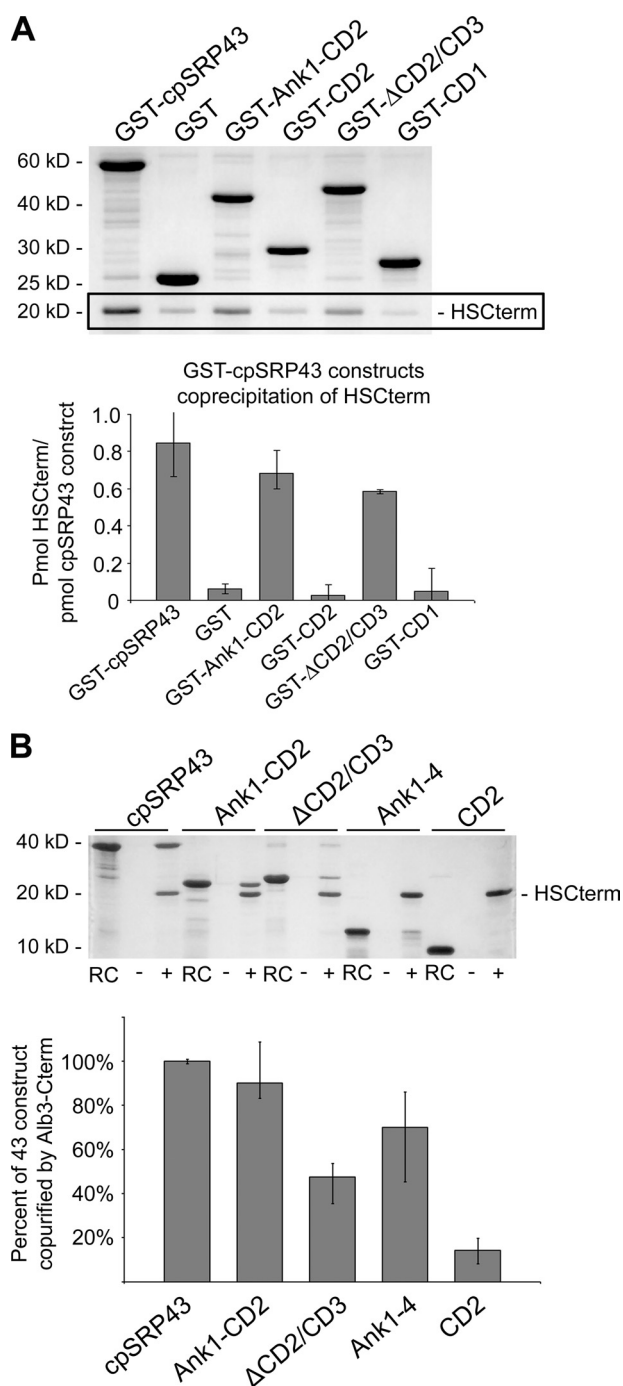
FIGURE 3. **Ankyrin region of cpSRP43 and Alb3-Cterm coprecipitate.** *A,* equimolar concentrations of GST or GST-43 construct were incubated with His-S$_{tag}$-Alb3-Cterm and then recovered using glutathione-Sepharose resin and eluted with SDS buffer. Eluates were analyzed by SDS-PAGE and Coomassie Blue staining. *B,* equimolar concentrations of His-S$_{tag}$-Alb3-Cterm were incubated with cpSRP43, His-Ank1-CD2, ΔCD2/CD3, His-Ank1–4, or His-CD2 and then recovered using S-protein-agarose resin and eluted with SDS buffer. *Lanes* show proteins precipitated by His-S$_{tag}$-Alb3-Cterm (+) compared with background binding to resin alone (−). *Lanes labeled RC* (recombinant control) show appropriate migration distance of each cpSRP43 construct into the gel. Eluates were analyzed as in *A.*

containing the ankyrin repeat region of cpSRP43 are also capable of copurifying Alb3-Cterm; GST-Ank1-CD2 and GST-ΔCD2/CD3 both copurified Alb3-Cterm at a ratio greater than ∼0.6 pmol of Alb3-Cterm per pmol of construct. Those con-

structs lacking the ankyrin repeats (CD1 and CD2) exhibit strong decreases in the amount of Alb3-Cterm copurified (less than 0.07 pmol of Alb3-Cterm per pmol of construct).

Likewise, we utilized a His-S$_{tag}$-Alb3-Cterm construct to verify an interaction between Alb3-Cterm and the ankyrin region of cpSRP43. cpSRP43 and constructs His-Ank1-CD2, ΔCD2/CD3, His-Ank1–4, and His-CD2 were incubated with His-S$_{tag}$-Alb3-Cterm and repurified using S-protein-agarose (Fig. 3*B*). Eluted proteins were separated by SDS-PAGE and visualized directly by staining with Coomassie Blue. Fig. 3*B* shows that cpSRP43, His-Ank1-CD2, ΔCD2/CD3, and His-Ank1–4 are specifically copurified with Alb3-Cterm, albeit to a lesser extent in the case of ΔCD2/CD3 and His-Ank1–4. Quantification from four separate assays shows that His-S$_{tag}$-Alb3-Cterm coprecipitates His-Ank1-CD2 at ∼90% the level of cpSRP43. His-Ank1–4 is coprecipitated at ∼70% of the level of cpSRP43. ΔCD2/CD3 was copurified at ∼50% of cpSRP43, whereas copurification of His-CD2 is only ∼15% of cpSRP43. Decreased copurification of His-Ank1–4 by Alb3-Cterm is likely due to the absence of CD2, which, in agreement with ITC (Fig. 2 and supplemental Table S1) and previous copurifications (Fig. 3*A*), provides minor additional strength to the interaction. The presence of CD1 reduces the amount of cpSRP43 construct copurified by Alb3-Cterm (∼70% by Ank1–4 compared with ∼50% by ΔCD2/CD3). It is interesting to speculate that CD1 may serve as a negative regulator of cpSRP43 binding to Alb3.

Alb3-Cterm Stimulates GTP Hydrolysis by cpSRP GTPases in a cpSRP43-dependent Manner—GTP binding and hydrolysis by cpSRP54/cpFtsY are critical for LHCP integration into the thylakoid membrane (12, 16). Given that the timing of GTP hydrolysis is carefully synchronized in SRP targeting to the endoplasmic reticulum as part of a mechanism to ensure that SRP is released from its receptor only after encountering an available translocase, it seems plausible that a similar mechanism to promote GTP hydrolysis only when Alb3 is available may involve cpSRP43 binding to Alb3-Cterm. To examine a possible influence of Alb3 on the GTP hydrolysis activity of cpSRP54/cpFtsY, we utilized a colorimetric assay that measures the release of P$_i$ by GTP hydrolysis as described previously (27, 44). The amount of P$_i$ released by 150 pmol each of cpSRP54 and cpFtsY (9.3 nmol of P$_i$ per h) does not appear to be changed by the addition of His-S$_{tag}$-Alb3-Cterm. However, in the presence of cpSRP43, GTP hydrolysis by cpSRP54 and cpFtsY is stimulated in a linear fashion with increasing amounts of Alb3-Cterm (Fig. 4). The addition of 6000 pmol of Alb3-Cterm to 150 pmol each of cpSRP43/cpSRP54/cpFtsY (40 mol of Alb3-Cterm, 1 mol of cpSRP43/cpSRP54/cpFtsY) results in a 5-fold stimulation in GTP hydrolysis (from 12.7 to 51.3 nmol of P$_i$). It is important to note that GTP hydrolysis assays were conducted in the absence of the signal peptide-mimicking detergent Nikkol, which is known to elevate the GTP hydrolysis activities of SRP/SRP receptor (46, 47) as well as cpSRP/cpFtsY (48). Regardless, our data demonstrate the ability of Alb3-Cterm to stimulate GTPase activity of cpSRP54 and cpFtsY is absolutely dependent on the presence of cpSRP43, which points to the cpSRP43-Alb3 interaction as representing a critical step in the recycling of cpSRP and its receptor.
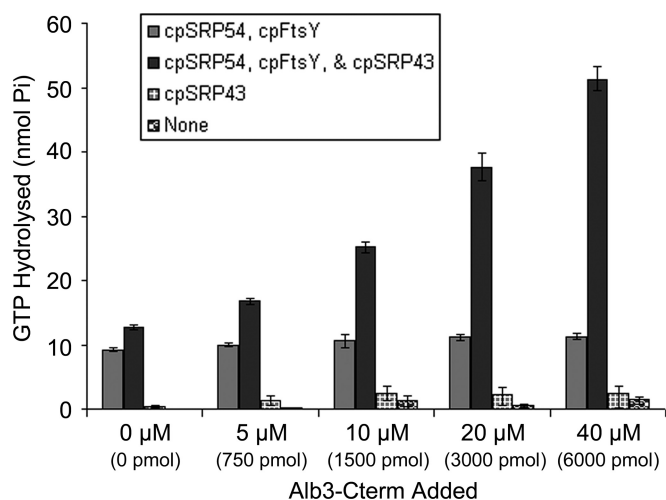
FIGURE 4. **Alb3-Cterm binding to cpSRP43 stimulates GTP hydrolysis by the cpSRP GTPases.** The effect of Alb3-Cterm on the GTP hydrolysis activity of cpSRP54 and cpFtsY was examined in the presence or absence of cpSRP43. Assays contained 150 pmol (1 μM final concentration) of cpSRP43, cpSRP54, and cpFtsY and 0–6000 pmol (0–40 μM final concentration) of His-S$_{tag}$-Alb3-Cterm as indicated with 2 mM GTP as described under "Experimental Procedures." GTPase activity resulting in the release of P$_i$ was determined according to González-Romo *et al.* (44) using known phosphate standards. The average and S.D. were calculated from three separate experiments.
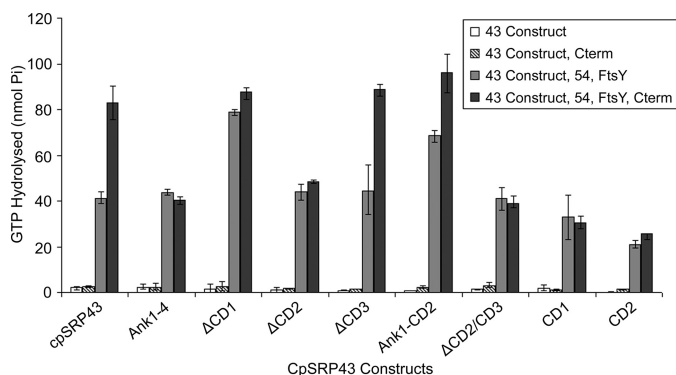
FIGURE 5. **Ankyrin region of cpSRP43 and chromodomain 2 are necessary for Alb3-Cterm stimulation of GTP hydrolysis by the cpSRP GTPases.** The effect of Alb3-Cterm on the GTP hydrolysis activity of cpSRP54 and cpFtsY was examined in the presence or absence of cpSRP43, His-Ank1–4, ΔCD1, ΔCD2, ΔCD3, His-Ank1-CD2, ΔCD2/CD3, His-CD1, and His-CD2. Assays contained 150 pmol (1 μM final concentration) of cpSRP43 construct, cpSRP54, and cpFtsY and 4000 pmol (27 μM final) of His-S$_{tag}$-Alb3-Cterm as indicated with 2 mM GTP. GTPase activity resulting in the release of P$_i$ was determined according to González-Romo *et al.* (44) using known phosphate standards. The average and S.D. were calculated from three separate experiments.

cpSRP43 Ankyrin Repeats and Chromodomain 2, but Not Chromodomain 3, Are Necessary for the Alb3-Cterm Stimulation of GTP Hydrolysis by the cpSRP GTPases—A construct corresponding to the Ank1-CD2 region of cpSRP43 substitutes for full-length cpSRP43 in promoting stimulation of GTP hydrolysis by Alb3-Cterm (Fig. 5). Moreover, only cpSRP43 constructs containing both the Ank repeat domain and CD2 (ΔCD1, ΔCD3, and Ank1-CD2) were able to replace cpSRP43 in the ability to respond to the addition of Alb3-Cterm. Binding of the Ank repeat domain of cpSRP43 to Alb3-Cterm is likely communicated to cpSRP54/cpFtsY through interaction of the CD2 domain of cpSRP43 with cpSRP54 (33, 34, 49). It is noteworthy that cpSRP43 constructs lacking CD1 (ΔCD1, His-Ank1-CD2) exhibit elevated levels of GTP hydrolysis in

the absence of Alb3-Cterm such that stimulation of GTP hydrolysis by addition of Alb3-Cterm is less pronounced. These observations are consistent with our previous work showing that CD1 serves as a negative regulator of GTP hydrolysis (27). Taken together, the data presented in Figs. 3 and 5 argue for a model in which Alb3 binding to the cpSRP43 Ank region is communicated by CD2 to cpSRP GTPases via a mechanism that reverses the negative GTPase regulation associated with CD1.

cpSRP43/Alb3-Cterm Interaction Plays a Role in the Separation of LHCP from cpSRP—It is well established that regulation of the GTPase cycle is a primary means of ensuring highly efficient and unidirectional SRP targeting. Membrane-bound ribosome-nascent chains associated with SRP and SRP receptor remain in the GTP-bound conformation in the absence of an active translocation channel (50), suggesting that the interaction with the translocon and release of the signal sequence are prerequisite for GTP hydrolysis. Similarly, the interaction of signal peptides with SRP·SRP receptor complex inhibits GTPase activity in the absence of an available Sec translocase (51, 52). We also observe a reduction in GTP hydrolysis by cpSRP54 and cpFtsY in the presence of cpSRP43 and L18.[5] Like cotranslationally targeted nascent polypeptides, LHCP must be released from cpSRP prior to or simultaneous with the recycling of the targeting components. The question lingers as to the events that initiate LHCP release from cpSRP. We took advantage of the fact that radiolabeled LHCP in complex with cpSRP43 and cpSRP54 can be detected as a soluble complex (termed transit complex) on nondenaturing gels (21, 32). If Alb3-Cterm binding to cpSRP43 is part of the mechanism to initiate LHCP release from cpSRP, we predict that transit complex formation and stability would be sensitive to the presence of Alb3-Cterm.

Fig. 6, *A* and *B*, shows that incubation of radiolabeled pLHCP with cpSRP43 and cpSRP54 reconstitutes formation of a cpSRP·LHCP transit complex, which migrates as a distinct band when examined using nondenaturing PAGE. In the absence of cpSRP, pLHCP remains in the sample well (not shown) as documented previously (32). The addition of His-S$_{tag}$-Alb3-Cterm to the transit complex assay following complex formation results in an upward shift in the radiolabeled LHCP signal such that most of the LHCP is found in the well at the highest concentration of Alb3-Cterm. To understand whether upward migration of LHCP stems from a shift of the entire LHCP·cpSRP transit complex or reflects an Alb3-Cterm-induced instability of transit complex, we used radiolabeled cpSRP43 or cpSRP54 to follow their relative migration. Whereas the migration of cpSRP43 and cpSRP54 in native gels was similarly shifted at all concentrations of Alb3-Cterm examined, increasing Alb3-Cterm concentrations caused LHCP to separate from the cpSRP components and accumulate in the well (Fig. 6*A*). Both the shift in migration of cpSRP components and the accumulation of LHCP in the well appeared specific to the influence of Alb3-Cterm because neither GST nor the CD3 domain of cpSRP43 as a recombinant protein affected transit

---

[5] N. E. Lewis, N. J. Marty, R. L. Henry, and R. L. Goforth, unpublished data.

A

HSCterm concentration (µM)

0 8.3 16.7 83.3   0 8.3 16.7 83.3   0 8.3 16.7 83.3

TC -

LHCP*   cpSRP43*   cpSRP54*

B

HSCterm concentration (µM)   CD3 concentration (µM)   GST concentration (µM)

0 1.7 3.3 5 6.7 8.3 16.7 25   0 4.2 8.3 16.7 33.3   0 4.2 8.3 16.7 33.3

TC -   TC -   TC -
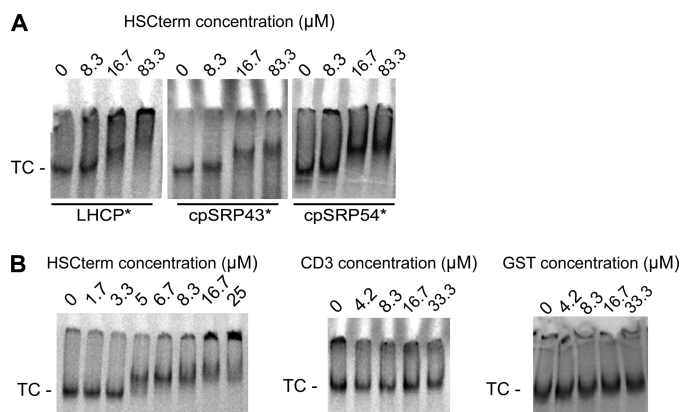
FIGURE 6. **Interaction of cpSRP43 and Alb3-Cterm destabilizes transit complex.** *A, in vitro* translated transit complex components (pLHCP, cpSRP43, and cpSRP54) were incubated in the presence of increasing concentrations (0–83.3 µM and 0–5000 pmol) of His-S_{tag}-Alb3-Cterm as indicated. Transit complex formation was examined using native PAGE and phosphorimaging for the radiolabeled component as indicated (*). *TC* indicates transit complex band. *B*, recombinant cpSRP43 and cpSRP54, in combination with *in vitro* translated and radiolabeled pLHCP, were used to form transit complex, which was monitored as in *A* after the addition of increasing concentrations (0–33.3 µM and 0–2000 pmol) of His-S_{tag}-Alb3-Cterm, GST, or CD3 as indicated. *TC* indicates transit complex band.

complex migration (Fig. 6*B*). This destabilization effect appears to involve formation of a slow migrating intermediate complex, which contains cpSRP54/cpSRP43/LHCP. Presumably, the slow migration of this intermediate represents transit complex bound to Alb3-Cterm. However, this remains to be confirmed. Another possibility is that binding of Alb3-Cterm to cpSRP43 in a transit complex state induces a conformational change, either in cpSRP43 individually or the transit complex as a species, leading to a shape/charge change that affects the migration of the complex into the nondenaturing gel.

Although the level of Alb3-Cterm required to observe changes in the transit complex are higher than anticipated, this could be expected if affinity of Alb3-Cterm for cpSRP43 is influenced by the lipid environment normally surrounding Alb3 or by cpSRP43 interaction partners, which differ at each step of the targeting pathway (*e.g.* affinity of Alb3-Cterm for cpSRP43 alone may be different from its affinity for cpSRP43 in transit complex with cpSRP54 and LHCP or in a cpSRP54·LHCP·cpFtsY complex at the membrane). Related to this possibility, Alb3-Cterm binding to cpSRP43 may also influence the affinity of cpSRP43 for its interaction partners (*e.g.* LHCP) as part of the mechanism that leads to unidirectional targeting of LHCP to Alb3. The ability of Alb3-Cterm to affect transit complex stability suggests there may be downstream effects on LHCP integration. However, studies involving the use of Alb3-Cterm to examine its influence on LHCP integration were inconclusive because of the ability of Alb3-Cterm to influence thylakoid membrane integrity.[5]

DISCUSSION

Previous work has established that the unique post-translational activities of an SRP targeting system in chloroplasts enable cpSRP to bind imported LHCP targeting substrates in the stroma and direct them to the thylakoid membrane, resulting in formation of a membrane complex containing cpSRP/

cpFtsY, bound substrate, and Alb3 (12, 17, 53). However, many of the mechanistic features underlying formation and disassembly of the membrane complex are not well understood. A possible role of cpSRP43 in membrane-localized targeting events was suggested by our previous work showing that cpSRP43 alone binds thylakoid membranes and is recovered in association with Alb3 (24). Data presented in this study indicate that the cpSRP43 binding of cpSRP54, LHCP, and Alb3 at distinct steps in the targeting pathway is used to communicate pathway progression of the targeting substrate to the evolutionarily conserved GTPases (cpSRP54/cpFtsY) such that GTPase activity is repressed until cpSRP43 interacts with an available Alb3 translocase. Together, our results support a model in which cpSRP43 serves as a translocon-sensing component to regulate the timing of membrane-associated steps in the post-translational cpSRP-dependent targeting pathway, *e.g.* transfer of substrate from cpSRP and recycling of SRP-targeting components.

Details of a cpSRP43-Alb3 interaction were reported recently and indicated that cpSRP43 chromodomains (CD2-CD3) form the binding interface with Alb3-Cterm (13). However, the low affinity reported between Alb3-Cterm and cpSRP43 (K_d 9.7 µM) or CD2-CD3 (K_d ~25 µM) led us to re-examine this interaction using a combination of approaches. Although our data confirm an interaction between cpSRP43 and Alb3-Cterm, the affinity appears to be in the nanomolar (K_d ~94 nM), not micromolar, range. The disparity between our findings and those reported likely emanate, in part, from the use of glycerol by Falk *et al.* (13) in ITC experiments, which contributes significantly to the heats of dilution and thereby influences the binding constant K_d calculation(s) (supplemental Fig. S2). Furthermore, although CD2 may contribute to the binding interface, our data (Figs. 2 and 3 and supplemental Table S1) comparing affinity of Alb3-Cterm for cpSRP43, Ank1-CD2, and CD2 suggest that the ankyrin repeats provide the primary interface for binding to Alb3-Cterm (K_d ~205 nM). In addition, although Falk *et al.* (13) state that the interaction with Alb3-Cterm requires both CD2 and CD3, it should be noted that CD3 is not required for integration of LHCP (27). *In vivo* data also indicates that CD2 does not play a critical role in targeting to Alb3, but instead it is restricted to SRP dimer formation and cpSRP43 chaperone activity (24–26).

Physiological significance of the interaction between cpSRP43 and Alb3-Cterm is supported by the ability of Alb3-Cterm peptide to stimulate GTP hydrolysis by cpSRP54/cpFtsY only in the presence of cpSRP43 and to promote release of LHCP from cpSRP in transit complex. cpSRP43 therefore appears to function as a mediator, linking the translocon, substrate, and cpSRP GTPases. *In vivo* studies have shown that LHCPs are predominantly routed via a cpSRP54 (cpFtsY)-dependent pathway but can be routed by a cpSRP54 (cpFtsY)-independent pathway in the absence of cpSRP54 (24). The cpSRP54-independent mechanism relies on cpSRP43, which is consistent with the ability of cpSRP43 to bind LHCP (28), function as an LHCP family-specific chaperone (25, 26), and interact with the Alb3 insertase (13, 24). It should be noted that although there are several possible roles for cpSRP54 in LHCP localization, *e.g.* substrate release from cpSRP43 or recycling of
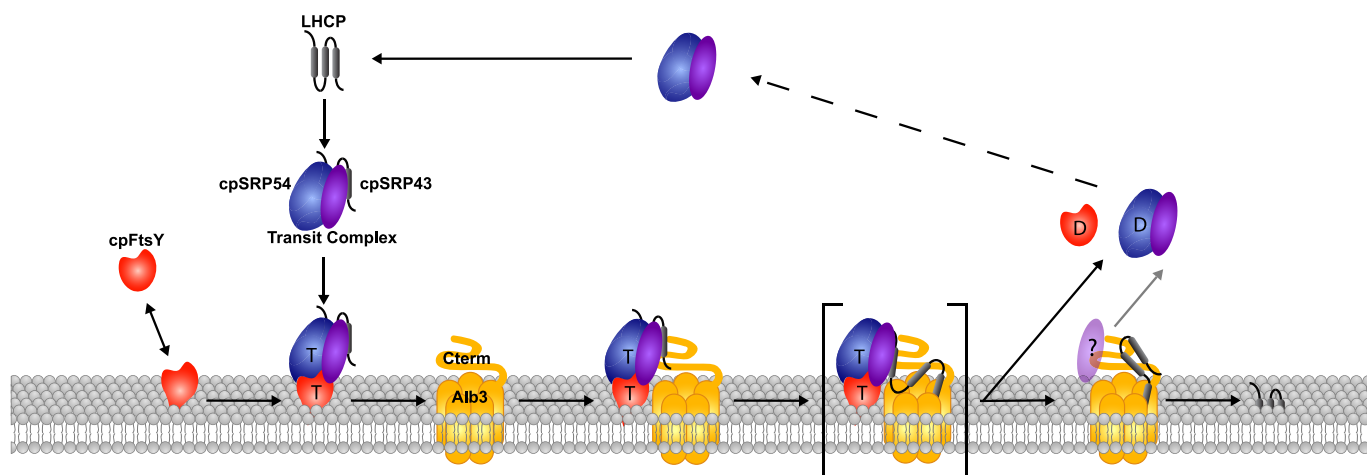
FIGURE 7. **Current cpSRP43-dependent targeting model.** Interactions with thylakoid membranes prime cpFtsY for binding cpSRP54 and GTP. Interactions with cpSRP43/LHCP prime cpSRP54 for binding GTP. The GTP-bound cpSRP43·LHCP·cpSRP54 complex associates with GTP-bound cpFtsY on thylakoid membranes. The membrane-associated complex is directed to Alb3 via an interaction between the Ank1–4 region of cpSRP43 and the C terminus of Alb3. cpSRP43 binding to the C terminus of Alb3 initiates LHCP release from cpSRP. LHCP, which acts as a negative regulator of hydrolysis, is released from cpSRP for insertion into thylakoids. In the absence of LHCP, interactions with thylakoid membranes, cpSRP43, and Alb3 trigger reciprocal stimulation of GTP hydrolysis by cpSRP54 and cpFtsY. GTP hydrolysis leads to dissociation of cpSRP43/54 and cpFtsY components from Alb3 and the thylakoid membrane. cpSRP43 may remain associated with Alb3 following departure of the GTPases from the membrane.

cpSRP43 from the membrane, it remains a possibility that cpSRP54-dependent differences in LHCP accumulation observed *in vivo* (54) occur at the level of targeting to Alb3.

It is also important to consider that the Ank region of cpSRP43 functions to bind the L18 motif in LHCP, an event critical to formation of a cpSRP·LHCP transit complex in stroma (27, 28, 30–32). This raises the possibility that binding of Alb3-Cterm to the Ank region of cpSRP43 is part of a mechanism to reduce cpSRP43 affinity for LHCP, thereby serving to promote release of LHCP from cpSRP only in the presence of an available Alb3. The ability of Alb3-Cterm peptide to destabilize the transit complex is consistent with this hypothesis (Fig. 6). Although our data support a model in which the Alb3 C terminus interacts with cpSRP43 to initiate LHCP release from cpSRP at the membrane, binding of the released targeting substrate to Alb3 remains to be demonstrated. However, the levels of Alb3-Cterm, relative to the level of cpSRP in the assay, required to destabilize the transit complex were higher than expected, based on the high affinity of Alb3-Cterm for cpSPR43 (Fig. 2*A* and supplemental Table S1). This may stem from Alb3-Cterm exhibiting a lower affinity for cpSRP43 in transit complex relative to cpSRP43 alone or in a cpSRP·LHCP·cpFtsY complex at the membrane. Affinity of Alb3-Cterm for cpSRP43 in cpSRP heterodimer was reported to be considerably reduced relative to cpSRP43 alone (13). Furthermore, release of LHCP in an *in vivo* environment is likely directly coupled to integration and would therefore require full-length Alb3 and lipid components. Regardless, the concentration-dependent ability of Alb3-Cterm (but not GST or CD3; Fig. 6) to destabilize the transit complex appears to take place through formation of a slow migrating intermediate containing at least cpSRP54/cpSRP43/LHCP. The formation and disappearance of this intermediate relative to the disappearance of transit complex and appearance of LHCP in the sample well (free from cpSRP) is consistent with the idea that formation of an intermediate is a required step during LHCP release from cpSRP. Considering the data shown

here and the current model for GTPase regulation of cytosolic SRPs (55), we propose the following model for cpSRP GTPase regulation (Fig. 7). Binding of cpSRP to LHCP to form transit complex primes cpSRP54 for binding GTP. Interactions with thylakoid membranes prime cpFtsY for binding cpSRP54 and GTP (36). The GTP-bound cpSRP43·LHCP·cpSRP54 transit complex in stroma associates with GTP-bound cpFtsY on thylakoid membranes. The membrane-associated complex is directed to Alb3 via an interaction between the Ank1–4 region of cpSRP43 and the C terminus of Alb3, which initiates LHCP release from cpSRP and GTP hydrolysis by cpSRP54/cpFtsY. In the absence of available Alb3, cpSRP/LHCP/cpFtsY remains in a membrane-associated complex because of an affinity of cpFtsY for lipids (36). GTP hydrolysis by cpSRP54 and cpFtsY leads to dissociation of cpSRP43/cpSRP54 and cpFtsY from Alb3. Our model, which incorporates general features from cotranslational SRP targeting systems, emphasizes a central role of cpSRP43 in soluble and membrane-targeting events because of its ability to bind Alb3 and initiate steps that stimulate GTP hydrolysis as well as reduce cpSRP affinity for LHCP-targeting substrate. We are currently working toward a greater understanding of the steps critical for LHCP release from cpSRP and recycling of soluble targeting components.

REFERENCES

1. Luirink, J., Samuelsson, T., and de Gier, J. W. (2001) *FEBS Lett.* **501,** 1–5
2. Yen, M. R., Harley, K. T., Tseng, Y. H., and Saier, M. H., Jr. (2001) *FEMS Microbiol. Lett.* **204,** 223–231
3. Stuart, R. A. (2002) *Biochim. Biophys. Acta* **1592,** 79–87
4. Dalbey, R. E., and Chen, M. (2004) *Biochim. Biophys. Acta* **1694,** 37–53
5. Yi, L., and Dalbey, R. E. (2005) *Mol. Membr. Biol.* **22,** 101–111
6. Kuhn, A., Stuart, R., Henry, R., and Dalbey, R. E. (2003) *Trends Cell Biol.* **13,** 510–516
7. Jiang, F., Yi, L., Moore, M., Chen, M., Rohl, T., Van Wijk, K. J., De Gier, J. W., Henry, R., and Dalbey, R. E. (2002) *J. Biol. Chem.* **277,** 19281–19288
8. van Bloois, E., Nagamori, S., Koningstein, G., Ullers, R. S., Preuss, M., Oudega, B., Harms, N., Kaback, H. R., Herrmann, J. M., and Luirink, J. (2005) *J. Biol. Chem.* **280,** 12996–13003

9. Preuss, M., Ott, M., Funes, S., Luirink, J., and Herrmann, J. M. (2005) *J. Biol. Chem.* **280,** 13004–13011

10. Jia, L., Dienhart, M., Schramp, M., McCauley, M., Hell, K., and Stuart, R. A. (2003) *EMBO J.* **22,** 6438–6447

11. Szyrach, G., Ott, M., Bonnefoy, N., Neupert, W., and Herrmann, J. M. (2003) *EMBO J.* **22,** 6448–6457

12. Moore, M., Goforth, R. L., Mori, H., and Henry, R. (2003) *J. Cell Biol.* **162,** 1245–1254

13. Falk, S., Ravaud, S., Koch, J., and Sinning, I. (2010) *J. Biol. Chem.* **285,** 5954–5962

14. Asakura, Y., Hirohashi, T., Kikuchi, S., Belcher, S., Osborne, E., Yano, S., Terashima, I., Barkan, A., and Nakai, M. (2004) *Plant Cell* **16,** 201–214

15. Hutin, C., Havaux, M., Carde, J. P., Kloppstech, K., Meiherhoff, K., Hoffman, N., and Nussaume, L. (2002) *Plant J.* **29,** 531–543

16. Tu, C. J., Schuenemann, D., and Hoffman, N. E. (1999) *J. Biol. Chem.* **274,** 27219–27224

17. Moore, M., Harrison, M. S., Peterson, E. C., and Henry, R. (2000) *J. Biol. Chem.* **275,** 1529–1532

18. Klimyuk, V. I., Persello-Cartieaux, F., Havaux, M., Contard-David, P., Schuenemann, D., Meiherhoff, K., Gouet, P., Jones, J. D., Hoffman, N. E., and Nussaume, L. (1999) *Plant Cell* **11,** 87–99

19. Schuenemann, D., Gupta, S., Persello-Cartieaux, F., Klimyuk, V. I., Jones, J. D., Nussaume, L., and Hoffman, N. E. (1998) *Proc. Natl. Acad. Sci. U.S.A.* **95,** 10312–10316

20. Schünemann, D. (2004) *Curr. Genet.* **44,** 295–304

21. Li, X., Henry, R., Yuan, J., Cline, K., and Hoffman, N. E. (1995) *Proc. Natl. Acad. Sci. U.S.A.* **92,** 3789–3793

22. Bacher, G., Lütcke, H., Jungnickel, B., Rapoport, T. A., and Dobberstein, B. (1996) *Nature* **381,** 248–251

23. Mandon, E. C., Jiang, Y., and Gilmore, R. (2003) *J. Cell Biol.* **162,** 575–585

24. Tzvetkova-Chevolleau, T., Hutin, C., Noël, L. D., Goforth, R., Carde, J. P., Caffarri, S., Sinning, I., Groves, M., Teulon, J. M., Hoffman, N. E., Henry, R., Havaux, M., and Nussaume, L. (2007) *Plant Cell* **19,** 1635–1648

25. Falk, S., and Sinning, I. (2010) *J. Biol. Chem.* **285,** 21655–21661

26. Jaru-Ampornpan, P., Shen, K., Lam, V. Q., Ali, M., Doniach, S., Jia, T. Z., and Shan, S. O. (2010) *Nat. Struct. Mol. Biol.* **17,** 696–702

27. Goforth, R. L., Peterson, E. C., Yuan, J., Moore, M. J., Kight, A. D., Lohse, M. B., Sakon, J., and Henry, R. L. (2004) *J. Biol. Chem.* **279,** 43077–43084

28. Tu, C. J., Peterson, E. C., Henry, R., and Hoffman, N. E. (2000) *J. Biol. Chem.* **275,** 13187–13190

29. Groves, M. R., Mant, A., Kuhn, A., Koch, J., Dübel, S., Robinson, C., and Sinning, I. (2001) *J. Biol. Chem.* **276,** 27778–27786

30. Jonas-Straube, E., Hutin, C., Hoffman, N. E., and Schünemann, D. (2001) *J. Biol. Chem.* **276,** 24654–24660

31. Stengel, K. F., Holdermann, I., Cain, P., Robinson, C., Wild, K., and Sinning, I. (2008) *Science* **321,** 253–256

32. DeLille, J., Peterson, E. C., Johnson, T., Moore, M., Kight, A., and Henry, R. (2000) *Proc. Natl. Acad. Sci. U.S.A.* **97,** 1926–1931

33. Hermkes, R., Funke, S., Richter, C., Kuhlmann, J., and Schünemann, D. (2006) *FEBS Lett.* **580,** 3107–3111

34. Kathir, K. M., Rajalingam, D., Sivaraja, V., Kight, A., Goforth, R. L., Yu, C., Henry, R., and Kumar, T. K. (2008) *J. Mol. Biol.* **381,** 49–60

35. Cline, K., Fulsom, D. R., and Viitanen, P. V. (1989) *J. Biol. Chem.* **264,** 14225–14232

36. Marty, N. J., Rajalingam, D., Kight, A. D., Lewis, N. E., Fologea, D., Kumar, T. K., Henry, R. L., and Goforth, R. L. (2009) *J. Biol. Chem.* **284,** 14891–14903

37. Yuan, J., Kight, A., Goforth, R. L., Moore, M., Peterson, E. C., Sakon, J., and Henry, R. (2002) *J. Biol. Chem.* **277,** 32400–32404

38. Woolhead, C. A., Thompson, S. J., Moore, M., Tissier, C., Mant, A., Rodger, A., Henry, R., and Robinson, C. (2001) *J. Biol. Chem.* **276,** 40841–40846

39. Cline, K., Henry, R., Li, C., and Yuan, J. (1993) *EMBO J.* **12,** 4105–4114

40. Arnon, D. I. (1949) *Plant Physiol.* **24,** 1–15

41. Chu, F., Shan, S. O., Moustakas, D. T., Alber, F., Egea, P. F., Stroud, R. M., Walter, P., and Burlingame, A. L. (2004) *Proc. Natl. Acad. Sci. U.S.A.* **101,** 16454–16459

42. Jelesarov, I., and Bosshard, H. R. (1999) *J. Mol. Recognit.* **12,** 3–18

43. Payan, L. A., and Cline, K. (1991) *J. Cell Biol.* **112,** 603–613

44. González-Romo, P., Sánchez-Nieto, S., and Gavilanes-Ruíz, M. (1992) *Anal. Biochem.* **200,** 235–238

45. Roselin, L. S., Lin, M. S., Lin, P. H., Chang, Y., and Chen, W. Y. (2010) *Biotechnol. J.* **5,** 85–98

46. Bradshaw, N., Neher, S. B., Booth, D. S., and Walter, P. (2009) *Science* **323,** 127–130

47. Zhang, X., Schaffitzel, C., Ban, N., and Shan, S. O. (2009) *Proc. Natl. Acad. Sci. U.S.A.* **106,** 1754–1759

48. Jaru-Ampornpan, P., Nguyen, T. X., and Shan, S. O. (2009) *Mol. Biol. Cell* **20,** 3965–3973

49. Sivaraja, V., Kumar, T. K., Leena, P. S., Chang, A. N., Vidya, C., Goforth, R. L., Rajalingam, D., Arvind, K., Ye, J. L., Chou, J., Henry, R., and Yu, C. (2005) *J. Biol. Chem.* **280,** 41465–41471

50. Song, W., Raden, D., Mandon, E. C., and Gilmore, R. (2000) *Cell* **100,** 333–343

51. Miller, J. D., and Walter, P. (1993) *CIBA Found. Symp.* **176,** 147–163

52. Rapiejko, P. J., and Gilmore, R. (1997) *Cell* **89,** 703–713

53. Kogata, N., Nishio, K., Hirohashi, T., Kikuchi, S., and Nakai, M. (1999) *FEBS Lett.* **447,** 329–333

54. Rutschow, H., Ytterberg, A. J., Friso, G., Nilsson, R., and van Wijk, K. J. (2008) *Plant Physiol.* **148,** 156–175

55. Shan, S. O., and Walter, P. (2005) *FEBS Lett.* **579,** 921–926

A Dynamic cpSRP43-Albino3 Interaction Mediates Translocase Regulation of Chloroplast Signal Recognition Particle (cpSRP)-targeting Components

Nathaniel E. Lewis, Naomi J. Marty, Karuppanan Muthusamy Kathir, Dakshinamurthy Rajalingam, Alicia D. Kight, Anna Daily, Thallapuranam Krishnaswamy Suresh Kumar, Ralph L. Henry and Robyn L. Goforth